Dynamics of binary mixtures in inhomogeneous temperatures

2008 J. Phys. A: Math. Theor. 41 105001

(http://iopscience.iop.org/1751-8121/41/10/105001)

IOP PUBLISHING JOURNAL OF PHYSICS A: MATHEMATICAL AND THEORETICAL

J. Phys. A: Math. Theor. **41** (2008) 105001 (13pp) doi:10.1088/1751-8113/41/10/105001

Dynamics of binary mixtures in inhomogeneous temperatures

G Gonnella[1], **A Lamura**[2] **and A Piscitelli**[1]

[1] Dipartimento di Fisica, Università di Bari and Istituto Nazionale di Fisica Nucleare, Sezione di Bari, via Amendola 173, 70126 Bari, Italy
[2] Istituto Applicazioni Calcolo, CNR, via Amendola 122/D, 70126 Bari, Italy

Received 5 October 2007, in final form 18 January 2008
Published 26 February 2008
Online at stacks.iop.org/JPhysA/41/105001

Abstract

A dynamical description for fluid binary mixtures with variable temperature and concentration gradient contributions to entropy and internal energy is given. By using mass, momentum and energy balance equations together with the standard expression for entropy production, a generalized Gibbs–Duhem relation is obtained which takes into account thermal and concentration gradient contributions. Then an expression for the pressure tensor is derived. As examples of applications, interface behavior and phase separation have been numerically studied in two dimensions neglecting the contributions of the velocity field. In the simplest case with a constant thermal gradient, the growth exponent for the averaged size of domains is found to have the usual value $z = 1/3$ and the domains appear elongated in the direction of the thermal gradient. When the system is quenched by contact with external walls, the evolution of temperature profiles in the system is shown and the domain morphology is characterized by interfaces perpendicular to the thermal gradient.

PACS numbers: 47.10.A−, 05.70.Ln, 44.35.+c, 64.75.Gh

1. Introduction

Fluid interfaces are characterized by finite thickness [1]. Since the pioneering work of van der Waals [2] on gas–liquid interfaces, theories with gradient concentration terms in free-energy density are commonly used to describe interfaces between fluids. They are also used in statistical mechanics of nonuniform states as, for example, in the Cahn–Hilliard model for phase transitions in binary alloys [3] and, more generally, in Landau–Ginzburg field theories [4]. Interfaces contribute to momentum and energy hydrodynamic equations through the expression of the stress tensor, as first recognized by Korteweg [5].

Usually, in the theories mentioned above, the temperature is assumed not varying in space, and gradient contribution to thermodynamic forces has been calculated under this condition [6, 7]. However, there are many relevant phenomena in fluid systems with the temperature

not homogeneous or where a heat flow occurs. This happens, for example, in the boiling process [8, 9], droplet motion under thermal gradients [10, 11], phase separation [12] with heat exchanges. Therefore, theories for non-equilibrium processes in fluids have to take into account both the thermal and the hydrodynamic effects.

In this paper, we generalize to binary mixtures a theory recently proposed by Onuki [10] for describing the dynamics of van der Waals fluids. In this theory, which further develops previous works by Antanovskii [13] and Español [14], the full set of thermo-hydrodynamic equations is derived for fluids with entropy and internal energy functionals including gradient terms. By assuming the usual expression for entropy production, a generalized Gibbs–Duhem relation taking into account the presence of interfaces was obtained. This allowed us to get an expression for the pressure tensor containing explicit contributions resulting from thermal gradients, which did not appear in previous theories of [13, 14].

In the case of binary mixtures, diffusion between different species has to be also considered together with other transport mechanisms [15]. We obtain, for systems with gradient concentration terms in internal energy and entropy, a generalized Gibbs–Duhem relation and explicit expressions for pressure tensor and other thermodynamic quantities. These expressions generalize to non-isothermal cases the relations given in [6] for binary mixtures. They could be conveniently used in the existing numerical schemes for the simulation of thermal fluids, as already done, for the case of van der Waals fluids, in [10, 16]. In this paper, as examples of applications, we study interface profile behavior and phase separation neglecting the effects of the velocity field. We consider the different cases with a fixed thermal gradient instantaneously imposed on the whole system or with thermal variations induced by contact with external walls. We show that the morphology of the phase separating patterns greatly differs in the two cases: domains grow with interfaces perpendicular to thermal gradients when the temperature evolves following its dynamical equation, while they are elongated in the direction of the gradient in the other case. We also show the effects of different heat conductivities.

The paper is organized as follows. In section 2 we will first set down the thermodynamics of our system; later, after having introduced the transport equations, we will derive the Gibbs–Duhem relation and the analytical expression for the pressure tensor. Section 3 will contain the numerical results obtained from the applications mentioned first with the conclusion to follow.

2. The model

2.1. Thermodynamics

We consider a binary mixture with components having number densities n_1 and n_2. The total density will be $n = n_1 + n_2$ while $\varphi = n_1 - n_2$ is the order parameter. A gradient in φ is expected to decrease the entropy, due to inhomogeneities, and to increase the internal energy. In order to take into account interface contributions, the coarse grained entropy and internal energy are defined as

$$S = \int \left[ns - \frac{C}{2} |\vec{\nabla}\varphi|^2 \right] \mathrm{d}\vec{r}, \tag{1}$$

$$E = \int \left[e + \frac{K}{2} |\vec{\nabla}\varphi|^2 \right] \mathrm{d}\vec{r} \tag{2}$$

where s and e are the entropy per particle and the internal energy density of the bulk of the mixture, respectively, while the parameters C and K weight the interface contributions. In the

microscopic derivation of [15], gradient terms only appear in the internal energy and, actually, in our simulations we will put $C = 0$. However, in the phenomenological treatment of this section, also in analogy with the formulation of [10], we have considered both the gradient terms.

To be more explicit we consider a system with

$$e = e^{(0)} + e_{\rm int} = e^{(0)} + \frac{\lambda n}{4}\left(1 - \frac{\varphi^2}{n^2}\right) \tag{3}$$

and

$$ns = ns^{(0)} + ns_{\rm mix} = ns^{(0)} + k_B[n\ln(n) - n_1\ln(n_1) - n_2\ln(n_2)] \tag{4}$$

where $ns^{(0)} = n_1 s_1^{(0)} + n_2 s_2^{(0)}$, $e^{(0)} = e_1^{(0)} + e_2^{(0)}$, $s_i^{(0)}$ and $e_i^{(0)}$ $(i = 1, 2)$ are the entropy per particle and the internal energy density of the two components separately considered, $s_{\rm mix}$ is the mean-field expression for the mixing entropy, $e_{\rm int}$ is the interaction energy with strength λ (see, e.g., [17] for more details). For example, if a component is described by the van der Waals equation, one has $s_i^{(0)}/k_B = d/2\ln T + \ln(1/(Dn) - 1)$, $e_i^{(0)} = dnk_BT/2 - Cn^2$ where C, D are constants and d is the space dimension. In the simulations of the following, with constant total density at the symmetric consolute critical point, it is enough to consider only the ideal terms in the above expressions.

A critical transition between a mixed phase and separated phases with concentration

$$\varphi_\pm = \pm\sqrt{3n^2(\lambda/2k_BT - 1)} \tag{5}$$

occurs at $k_BT_c = \lambda/2$. The parameters C, K are related to the surface tension σ. For a system with free energy $F = \int\left(\psi(n,\varphi,T) + \frac{1}{2}M|\vec{\nabla}\varphi|^2\right)\mathrm{d}\vec{r}$, it is defined by

$$\sigma = \int \mathrm{d}y\left[\frac{M}{2}\left(\frac{\partial\varphi}{\partial y}\right)^2 + \psi(n,\varphi,T) - \psi(n,\varphi_\pm,T)\right] \tag{6}$$

where the integral is calculated along the normal to a flat interface. In our case $\psi(n,\varphi,T) = e - Tns$ and $M = K + CT$. In the φ^4-approximation, the dependence of ψ on φ reduces to $V(\varphi) = \frac{a}{2}\varphi^2 + \frac{b}{4}\varphi^4$, with $a = \frac{k_BT}{n} - \frac{\lambda}{2n}$ and $b = \frac{k_BT}{3n^3}$, and it comes out that $\sigma = \frac{2}{3}\sqrt{\frac{-2a^3M}{b^2}}$ [1].

Maximization of S under fixed total density $\int \mathrm{d}\vec{r}\,n$, given composition $\int \mathrm{d}\vec{r}\,\varphi$ and total internal energy E, leads to the equilibrium condition with constant temperature and chemical potentials. The unconditional variational problem consists in maximizing with respect to n, φ and $e^{(0)}$ the functional

$$S - \frac{1}{\vartheta}\int \mathrm{d}\vec{r}\left[e + \frac{K}{2}|\vec{\nabla}\varphi|^2\right] - \chi\int \mathrm{d}\vec{r}\,n - \xi\int \mathrm{d}\vec{r}\,\varphi \tag{7}$$

where Lagrangian multipliers have been introduced.

The first relation, obtained by differentiating the above expression with respect to $e^{(0)}$ at constant n and φ and observing that $(\delta S/\delta e^{(0)})_{n,\varphi} = (\delta S/\delta e)_{n,\varphi}$, is

$$0 = \left(\frac{\delta S}{\delta e}\right)_{n,\varphi} - \frac{1}{\vartheta} \tag{8}$$

which allows us to identify ϑ with the temperature T, as usually in statistical mechanics [17]. Moreover, functionally deriving (7) with respect to n and φ, one obtains

$$0 = \frac{\delta S}{\delta n} - \frac{1}{\vartheta}\frac{\delta}{\delta n}\int \mathrm{d}\vec{r}\left[\frac{\lambda n}{4}\left(1 - \frac{\varphi^2}{n^2}\right)\right] - \chi \tag{9}$$

$$0 = \frac{\delta S}{\delta \varphi} + \frac{\lambda \varphi}{2\vartheta n} + \frac{1}{\vartheta} K \nabla^2 \varphi - \xi \tag{10}$$

so that, with

$$\mu_i^{(0)} = -T \left(\frac{\partial n_i s_i^{(0)}}{\partial n_i} \right)_{e_i^{(0)}, n_{j \neq i}} \tag{11}$$

being the chemical potential of the component i individually considered, it results

$$\chi = -\frac{\mu_1^{(0)}}{2T} - \frac{\mu_2^{(0)}}{2T} + k_B \ln(n) - \frac{k_B}{2} \ln\left(\frac{n+\varphi}{2}\right) - \frac{k_B}{2} \ln\left(\frac{n-\varphi}{2}\right) - \frac{\lambda}{4T}\left(1 + \frac{\varphi^2}{n^2}\right) \tag{12}$$

and

$$\xi = -\frac{\mu_1^{(0)}}{2T} + \frac{\mu_2^{(0)}}{2T} - \frac{k_B}{2} \ln\left(\frac{n+\varphi}{2}\right) + \frac{k_B}{2} \ln\left(\frac{n-\varphi}{2}\right) + C \nabla^2 \varphi + \frac{\lambda \varphi}{2Tn} + \frac{K \nabla^2 \varphi}{T}. \tag{13}$$

This leads to the following expressions for the coexistence values for the equilibrium chemical potentials $\mu_i \equiv (\delta S / \delta n_i)_{\widehat{e}, n_{j \neq i}}$ of the two components in the mixture

$$\mu_1 = -T(\chi + \xi) = \mu_1^{(0)} + k_B T \ln(x_1) + \lambda x_2 - \frac{e_{\text{int}}}{n} - M \nabla^2 \varphi = \text{const} \tag{14}$$

$$\mu_2 = -T(\chi - \xi) = \mu_2^{(0)} + k_B T \ln(x_2) + \lambda x_1 - \frac{e_{\text{int}}}{n} + M \nabla^2 \varphi = \text{const} \tag{15}$$

with $x_i = n_i / n$.

We follow the approach of [10] to describe non-equilibrium behavior. We define the local temperature, generalizing the relation (8), by

$$\frac{1}{T} = \left(\frac{\delta S}{\delta e} \right)_{n, \varphi} = n \left(\frac{\partial s}{\partial e} \right)_{n, \varphi} \tag{16}$$

and the chemical potential difference μ as

$$\mu = -T \left(\frac{\delta S}{\delta \varphi} \right)_{\widehat{e}, n} \tag{17}$$

where

$$\widehat{e} = e + \frac{K}{2} |\, \overrightarrow{\nabla} \varphi|^2 \tag{18}$$

is the total internal energy density which includes also gradient contributions.

Since the functional derivative (17) is defined at constant $\widehat{e}$, a Lagrange multiplier field relative to $\widehat{e}$ has to be introduced which can be identified with the temperature of equation (16). Equation (17) can be rewritten as

$$\mu = -T \left\{ \frac{\delta}{\delta \varphi} \int \mathrm{d}\, \overrightarrow{r} \left[ns - \frac{1}{2} C |\, \overrightarrow{\nabla} \varphi|^2 - \frac{1}{T(\overrightarrow{r})} \left(e + \frac{K}{2} |\, \overrightarrow{\nabla} \varphi|^2 \right) \right] \right\}_{e^{(0)}, n} \tag{19}$$

and then, by using (4), (11) and performing the functional derivative, one obtains

$$\mu = \frac{\mu_1^{(0)}}{2} - \frac{\mu_2^{(0)}}{2} + \frac{k_B T}{2} \ln\left(\frac{n+\varphi}{n-\varphi}\right) - \frac{\lambda \varphi}{2n} - T\, \overrightarrow{\nabla} \cdot \left(\frac{M}{T} \overrightarrow{\nabla} \varphi \right) \tag{20}$$

which can be re-expressed as $\mu = (\mu_1 - \mu_2)/2$ with

$$\mu_{1/2} = \mu_{1/2}^{(0)} + k_B T \ln(x_{1/2}) + \lambda x_{2/1}^2 \mp T\, \overrightarrow{\nabla} \cdot \left(\frac{M}{T} \overrightarrow{\nabla} \varphi \right). \tag{21}$$

This reduces to equations (14)–(15) at constant temperature. μ_i can also be directly obtained by $\mu_i = \left(\frac{\delta S}{\delta n_i} \right)_{n_{j \neq i}, \widehat{e}}$. In the general case one has

$$\mu = -T \left[\frac{\partial (ns)}{\partial \varphi} - \frac{1}{T} \frac{\partial e}{\partial \varphi} + \overrightarrow{\nabla} \cdot \left(\frac{M}{T} \overrightarrow{\nabla} \varphi \right) \right]. \tag{22}$$

2.2. Hydrodynamic equations

In the context established by (1), (2), (16), (17) we pass to consider the dynamical equations. For a binary mixture the classical conservation equations of mass, momentum and energy in terms of the densities n and φ take the form [18]

$$\frac{\partial n}{\partial t} = -\partial_i(n v_i), \tag{23}$$

$$\frac{\partial \varphi}{\partial t} = -\partial_i(\varphi v_i) - 2\partial_i J_i^d, \tag{24}$$

$$n\frac{\mathrm{d}v_j}{\mathrm{d}t} = -\partial_i(\Pi_{ij} - \sigma_{ij}), \tag{25}$$

$$\frac{\partial \widehat{e}}{\partial t} = -\partial_i(\widehat{e} v_i) - (\Pi_{ij} - \sigma_{ij})\partial_i v_j - \partial_i J_i^q, \tag{26}$$

where $\overrightarrow{v}$ is the barycentric velocity field, ζ is the bulk viscosity, η is the shear viscosity. Moreover, $\overrightarrow{J_d}$ is the diffusion current, Π_{ij} is the reversible stress tensor, $\sigma_{ij} = \eta(\partial_i v_j + \partial_j v_i) + (\zeta - 2\eta/d)\delta_{ij}\partial_k v_k$ is the dissipative stress tensor and $\overrightarrow{J_q}$ is the heat current.

2.3. Pressure tensor and the generalized Gibbs–Duhem relation

An expression for the pressure tensor can be obtained assuming the usual form for the entropy production [4, 18]

$$\Sigma = -\frac{1}{T}\overrightarrow{\nabla}\cdot\overrightarrow{J_q} + \frac{1}{T}\sigma_{ik}\partial_k v_i + \frac{2\mu}{T}\overrightarrow{\nabla}\cdot\overrightarrow{J_d} \tag{27}$$

which can be rewritten in our formalism as

$$\Sigma = -\left(\frac{\delta S}{\delta \widehat{e}}\right)_{n,\varphi}\partial_i J_i^q + \left(\frac{\delta S}{\delta \widehat{e}}\right)_{n,\varphi}\sigma_{ik}\partial_k v_i - 2\left(\frac{\delta S}{\delta \varphi}\right)_{\widehat{e},n}\partial_i J_i^d. \tag{28}$$

By substituting equations (23), (24) and (26) into the general expression

$$\frac{\partial S}{\partial t} = \int \mathrm{d}\overrightarrow{r}\left\{\left(\frac{\delta S}{\delta n}\right)_{\widehat{e},\varphi}\left(\frac{\partial n}{\partial t}\right) + \left(\frac{\delta S}{\delta \widehat{e}}\right)_{n,\varphi}\left(\frac{\partial \widehat{e}}{\partial t}\right) + \left(\frac{\delta S}{\delta \varphi}\right)_{\widehat{e},n}\left(\frac{\partial \varphi}{\partial t}\right)\right\} \tag{29}$$

gives

$$\begin{aligned}\frac{\partial S}{\partial t} = \int \mathrm{d}\overrightarrow{r}\Bigg\{&-\left(\frac{\delta S}{\delta n}\right)_{\widehat{e},\varphi}\partial_i(n v_i) - \left(\frac{\delta S}{\delta \widehat{e}}\right)_{n,\varphi}\partial_i(\widehat{e} v_i) - \left(\frac{\delta S}{\delta \widehat{e}}\right)_{n,\varphi}\partial_i J_i^q - \left(\frac{\delta S}{\delta \widehat{e}}\right)_{n,\varphi}\Pi_{ij}\partial_i v_j \\ &+ \left(\frac{\delta S}{\delta \widehat{e}}\right)_{n,\varphi}\sigma_{ij}\partial_i v_j + \left(\frac{\delta S}{\delta \varphi}\right)_{\widehat{e},n}\left[-\partial_i(\varphi v_i) - 2\partial_i J_d^i\right]\Bigg\}.\end{aligned} \tag{30}$$

Using

$$\left(\frac{\delta S}{\delta \widehat{e}}\right)_{n,\varphi} = \left(\frac{\delta S}{\delta e}\right)_{n,\varphi} = \frac{1}{T} \tag{31}$$

and comparing (30) with (28), one obtains

$$\overrightarrow{\nabla}\cdot\left(\frac{\Pi}{T}\right) = -n\overrightarrow{\nabla}\left(\frac{\delta S}{\delta n}\right)_{\widehat{e},\varphi} - \widehat{e}\overrightarrow{\nabla}\left(\frac{\delta S}{\delta \widehat{e}}\right)_{n,\varphi} - \varphi\overrightarrow{\nabla}\left(\frac{\delta S}{\delta \varphi}\right)_{\widehat{e},n} \tag{32}$$

which represents a generalized Gibbs–Duhem relation for binary mixtures taking into account the presence of interface gradient contributions to the free energy.

Then, by using (1), (3), (4) and (18) to calculate the following derivatives,

$$\left(\frac{\delta S}{\delta n}\right)_{\widehat{e},\varphi} = -\frac{\mu_1^{(0)}}{2T} - \frac{\mu_2^{(0)}}{2T} + k_B \ln\left(\frac{2n}{\sqrt{n^2-\varphi^2}}\right) - \frac{\lambda}{4\vartheta}\left(\frac{\varphi^2}{n^2}+1\right) \tag{33}$$

$$\left(\frac{\delta S}{\delta \varphi}\right)_{\widehat{e},n} = -\frac{\mu_1^{(0)}}{2T} + \frac{\mu_2^{(0)}}{2T} - \frac{k_B}{2}\ln\left(\frac{n+\varphi}{n-\varphi}\right) + \frac{\lambda\varphi}{2nT} + \overrightarrow{\nabla}\cdot\left(\frac{M}{T}\overrightarrow{\nabla}\varphi\right) \tag{34}$$

$$\left(\frac{\delta S}{\delta \widehat{e}}\right)_{\varphi,n} = \frac{1}{T} = \left(\frac{\partial\left(n_1 s_1^{(0)}\right)}{\partial e}\right)_{n,\varphi} + \left(\frac{\partial\left(n_2 s_2^{(0)}\right)}{\partial e}\right)_{n,\varphi}, \tag{35}$$

and by substituting these expressions into equation (32), it is possible to demonstrate by direct algebraic manipulations that the Gibbs–Duhem equation is verified by a pressure tensor Π_{ij} having the form

$$\Pi_{ij} = \left(p - M\varphi\nabla^2\varphi - M\frac{|\overrightarrow{\nabla}\varphi|^2}{2} - T\varphi\overrightarrow{\nabla}\varphi\cdot\overrightarrow{\nabla}\left(\frac{M}{T}\right)\right)\delta_{ij} + M\partial_i\varphi\partial_j\varphi \tag{36}$$

where $p = -\psi + n\partial\psi/\partial n + \varphi\partial\psi/\partial\varphi$ with ψ defined after equation (6). In this derivation the standard Gibbs–Duhem relation for bulk thermodynamic quantities has been also used.

Now, having calculated the explicit expressions of the pressure tensor and of the chemical potential, the dynamical equations are completely set up if phenomenological expressions for $\vec{J}_q$, $\vec{J}_d$ are also given. A natural choice is [18]

$$\overrightarrow{J}_d = -\mathcal{L}_{11}\overrightarrow{\nabla}\left(\frac{\mu}{T}\right) + \mathcal{L}_{12}\overrightarrow{\nabla}\left(\frac{1}{T}\right), \tag{37}$$

$$\overrightarrow{J}_q = -\mathcal{L}_{21}\overrightarrow{\nabla}\left(\frac{\mu}{T}\right) + \mathcal{L}_{22}\overrightarrow{\nabla}\left(\frac{1}{T}\right). \tag{38}$$

In general the entropy production is written as a sum of products of flows and thermodynamic forces with the flows expressed as linear functions of the thermodynamic forces. As the variation of entropy is always positive or zero, the bilinear form defined by the matrix of elements $\mathcal{L}_{ij}$ must be positive defined and this implies for the phenomenological coefficients that $\mathcal{L}_{11} > 0$, $\mathcal{L}_{22} > 0$ and $\mathcal{L}_{11}\mathcal{L}_{22} - \mathcal{L}_{12}\mathcal{L}_{21} > 0$. Following [15, 18] we can assume that $\mathcal{L}_{11} = Tl_{11}$ and $\mathcal{L}_{22} = T^2 l_{22}$ with l_{11} and l_{22} constant. This would give the usual diffusion equation for the temperature in a homogeneous system where l_{22} is the heat conductivity.

We observe that the above choice of flows is coherent with the entropy production expression

$$\Sigma = \overrightarrow{J}_q\cdot\overrightarrow{\nabla}\left(\frac{1}{T}\right) - \overrightarrow{J}_d\cdot\overrightarrow{\nabla}\left(\frac{\mu_1-\mu_2}{T}\right) + \frac{1}{T}\sigma_{ik}\partial_k v_i \tag{39}$$

that can be obtained rearranging the integral of equation (27) by an integration by parts.

3. Results

In this section we consider applications of the theory previously derived in simple cases with constant thermal gradient or studying the combined evolution of the concentration and temperature fields neglecting only the contribution of the velocity field. We will show examples of stationary interface profiles and profile evolution after a temperature jump. Then we will

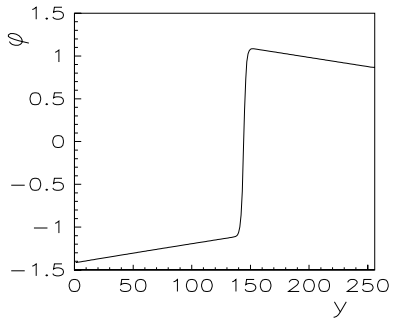

Figure 1. Equilibrium profile of φ in a system with $T_u = 0.4$, $T_l = 0.3$ ($T_C = 0.5$). The hot wall is on the right.

study phase separation for different values of the heat conductivity. The dynamics of the system will be described by the diffusion and energy equations (24), (26) with the diffusion and heat currents (37), (38) where we have set $\vec{v} = 0$. The chemical potential is derived from a free energy with $\psi(n, \varphi, T) = e - k_B T\left[n \ln(n) - \frac{n+\varphi}{2} \ln\left(\frac{n+\varphi}{2}\right) - \frac{n-\varphi}{2} \ln\left(\frac{n-\varphi}{2}\right)\right]$, $e = AT + \frac{\lambda n}{4}\left(1 - \frac{\varphi^2}{n^2}\right)$ where we have expanded the logarithmic terms up to fourth power and A is a constant. We have put $n = 1$, $A = 1$, $\lambda = 1$, $C = 0$, $K = 0.35$, $k_B = 1$ so that $T_c = 0.5$. We have also set $l_{12} = 0$. Recall that $\widehat{e}$ is defined in equation (18), μ can be calculated for example starting from (22) and ψ is defined after equation (6). We first give few details on the procedure used in our simulations.

3.1. Numerical method

Equations (24) and (26) are numerically integrated by using an explicit Euler scheme on a lattice of size $L_x \times L_y$ with time step Δt. The spatial differential operators are computed by a second-order finite difference scheme with spacing Δx. Concerning the mesh step, our choice for Δx was such that the smallest length scale in our problem (the interface width) was well resolved in terms of Δx and the results were mesh independent. The time step was small enough to ensure numerical stability. We assume periodic boundary conditions along the x-direction and place walls at the upper and lower rows of the lattice kept at fixed temperatures T_u and T_l, respectively, with $T_u > T_l$ (from now on the subscripts u and l will denote quantities computed at the upper and lower rows of the system). For the order parameter φ at walls we adopt neutral wetting which means that $\vec{a} \cdot \vec{\nabla}\varphi|_{y=0,L_y} = 0$, where $\vec{a}$ is the inward normal unit vector at the boundaries. We also require that $\vec{a} \cdot \vec{\nabla}(\nabla^2\varphi)|_{y=0,L_y} = 0$ to enforce strict conservation of the order parameter. In the following we will use $\Delta x = 1$, $\Delta t = 0.001$.

3.2. Interface profiles

In this section we neglect the contribution of equation (26). The temperature is kept fixed at each lattice site and varies only along the y-direction with a constant temperature gradient $\alpha = (T_u - T_l)/L_y$. In figure 1 we show the profile of φ for a system with a temperature varying between $T_u = 0.4$ and $T_l = 0.3$. This is obtained by finding the stationary solution of equation (24) for a one-dimensional system of size $L_x \times L_y = 1 \times 256$ starting from a step configuration with $\varphi(y) = \varphi_+(T = 0.4)$ (see equation (5)) when $L_y/2 \leqslant y \leqslant L_y$ and $\varphi(y) = \varphi_-(T = 0.3)$ for $0 \leqslant y < L_y/2$. The temperature gradient is then $\alpha = 0.00039$. The parameter l_{11} is set to 10. We see that the value of the field φ in the two phases is not

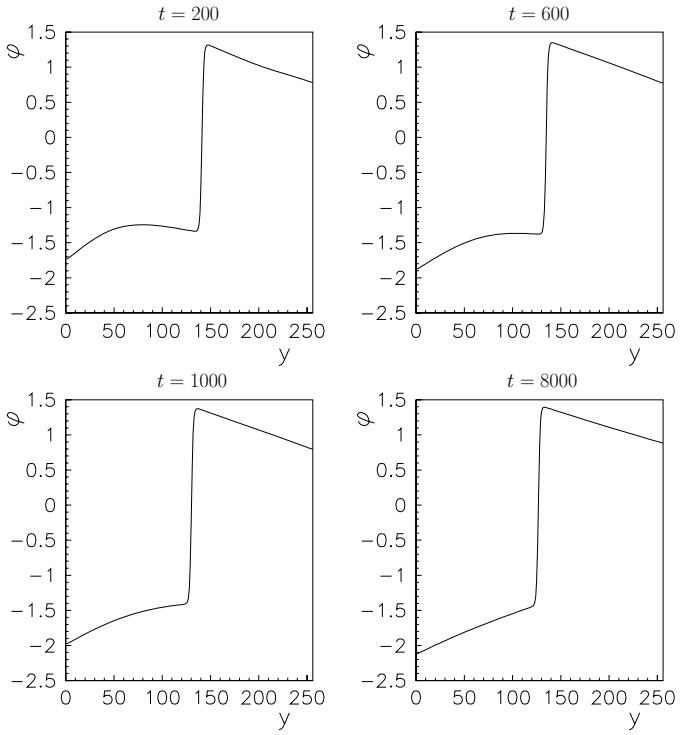

Figure 2. Profile of φ at consecutive times in a system quenched from $T_l = 0.3$ to $T_l = 0.2$ with T_u kept fixed at 0.4. The hot wall is on the right.

constant and non-monotonous respecting the temperature dependence given in equation (5). The interface has a width of about 6 lattice spacings. The system was then suddenly cooled at $T_l = 0.2$ doubling α. The evolution of the interface profile toward the new equilibrium state is shown in figure 2. The only peculiar feature to observe is that the concentration profile close to the cold wall evolves forming a shoulder which relaxes to a linear shape at later times.

3.3. Phase separation

We have studied the spinodal decomposition of symmetric systems, initially in a disordered state with the order parameter φ randomly distributed in the range $[-0.01, 0.01]$, quenched by instantaneously changing the temperature field to values below the critical point or by contact with cold walls. In the first case, equation (24) has been studied alone, while, in the second situation, the evolution of the temperature in the system is given by considering equation (26) too.

In figure 3 we show a sequence of configurations for the case with $l_{11} = 10, T_u = 0.4, T_l = 0.05$ on a lattice with size $L_x \times L_y = 1024 \times 1024$ at the fixed temperature gradient $\alpha = 0.00034$. We have also studied a system of size $L_x \times L_y = 2048 \times 2048$ for the same set of parameters thus having $\alpha = 0.00017$. The main effect observed is that at lower temperatures domains grow faster, while we did not find any relevant effect due to different thermal gradients. By averaging in a region of width $5\Delta x$ close to the walls at times $t = 4000, 6000, 8000$, we measured the width of domains along the walls. We found 2.02 for the ratio of domains' width at the bottom and top sides. In diffusive phase separation the

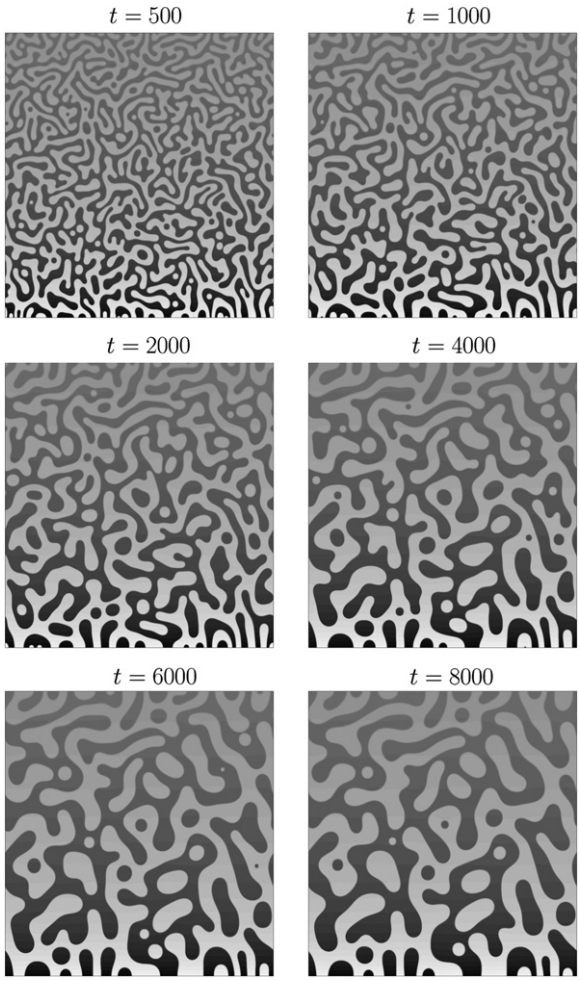

Figure 3. Contour plots of φ at consecutive times during phase separation on a system of size 1024×1024 with $T_u = 0.4$, $T_l = 0.05$ and constant temperature gradient profile. Cold and hot walls are placed at the bottom and top sides, respectively. Gray scaling from white $\rightarrow$ black corresponds to maximum $\varphi \rightarrow$ minimum φ.

typical size of domains grows as $R(t) \sim (\sigma t)^{1/3}$ [19]. Since the surface tension is higher at lower temperature, domains are expected to grow faster on colder walls but we found only a qualitative agreement with this law.

The average size $R(t)$ of domains has been calculated as the inverse of the first moment of the spherically averaged structure factor

$$R(t) = \frac{\int C(k,t)\,\mathrm{d}k}{\int kC(k,t)\,\mathrm{d}k}, \tag{40}$$

where $k = |\vec{k}|$ is the modulus of the wave vector in Fourier space and

$$C(k,t) = \langle \tilde{\varphi}(\vec{k},t)\tilde{\varphi}(-\vec{k},t)\rangle \tag{41}$$

with $\tilde{\varphi}(\vec{k},t)$ the spatial Fourier transform of the order parameter $\varphi(\vec{r},t)$. The angle brackets denote an average over a shell in Fourier space at fixed k. In principle, in equation (41)

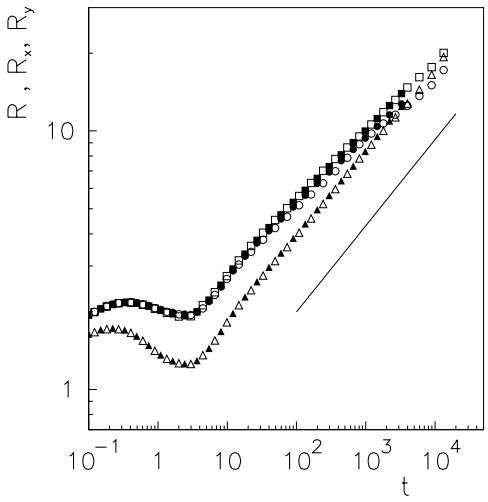

Figure 4. Average sizes of domains $R(\triangle)$, $R_x(\circ)$, $R_y(\square)$ as a function of time for two systems of size 1024×1024 (empty symbols) and 2048×2048 (filled symbols) with $T_u = 0.4$ and $T_l = 0.05$ and constant temperature gradient profile. The straight line is a guide to the eye and has a slope 1/3.

one should also perform an ensemble average over different initial conditions. However, for large system sizes as here, a self-averaging property can be generally assumed [19]. We also measure the domain size in the two spatial directions as

$$R_x(t) = \frac{\int \mathrm{d}\vec{k} C(\vec{k}, t)}{\int \mathrm{d}\vec{k} |k_x| C(\vec{k}, t)} \tag{42}$$

and the analogue R_y for the y-direction.

We looked at the global behavior of the domain size and for the spherically averaged size we found the growth law $R \sim t^{1/3}$ with R_y growing faster than R_x as shown in figure 4, showing the presence of anisotropy effects. From our results it seems to be plausible that the temperature gradient does not change the algebraic form of the growth law, but rather it may change the amplitude of R, R_x and R_y. This is confirmed by the results on the larger system also shown in figure 4 where the temperature gradient is halved with respect to the previous case. R_x and R_y grow with the same behavior with a slightly different amplitude.

We now show the effects of the temperature evolution, as described by equation (26), on the morphology of phase separation. Our choice of internal energy includes a term directly proportional to the temperature that can be therefore directly obtained by the integration of equation (26). We consider two cases, with $l_{22} = 10$ and $l_{22} = 100$. l_{11} is always kept fixed to 10 and the wall temperatures are $T_u = 0.4$, $T_l = 0.225$. The lattice size is $L_x \times L_y = 512 \times 512$. The evolution of the temperature across the system is shown for the first case at smaller heat conductivity in figure 5. The corresponding domain evolution is shown in figure 6. At the time $t = 250$ of our simulations, domains with well-defined interfaces can be observed close to the walls while in the central region the system is still in the disordered phase. Due to the neutral wetting condition, domains start to form with interfaces perpendicular to the walls but, moving toward the middle of the system, they grow oriented in the other direction. At $t = 1250$ phase separation has occurred in larger regions but in the middle of the system the disordered phase can still be observed. At successive times, a stack of domains perpendicular to the temperature gradient can be observed in all the systems except close to the boundary

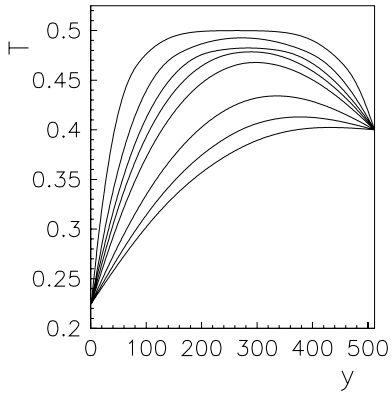

Figure 5. Temperature profiles across the system averaged along the x-direction with $T_u = 0.4$, $T_l = 0.225$ and $l_{22} = 10$ at times $t = 250, 750, 1250, 1750, 2500, 5000, 7500, 10\,000$ (from top to bottom).

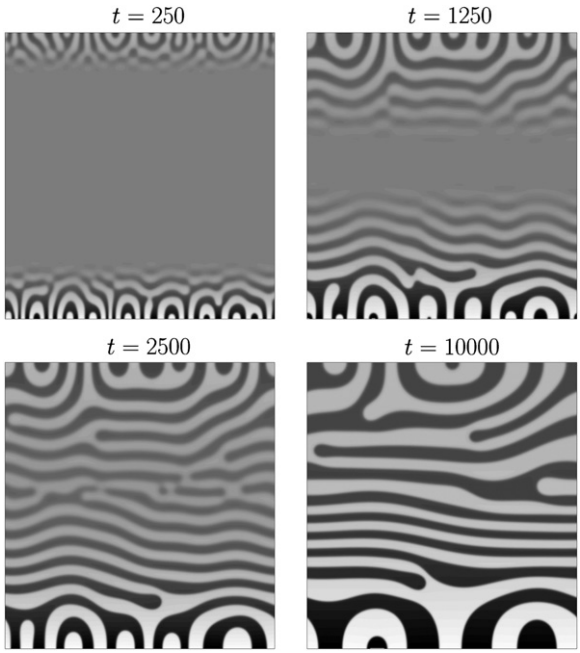

Figure 6. Contour plots of φ at consecutive times during phase separation on a system of size 512×512 with $T_u = 0.4$ and $T_l = 0.225$ and $l_{22} = 10$. Cold and hot walls are placed at the bottom and top sides, respectively. Gray scaling from white $\rightarrow$ black corresponds to maximum $\varphi \rightarrow$ minimum φ.

regions. These domains are characterized by a transversal width which grows with time but our statistics does not allow us to establish a quantitative law for this growth.

Going at higher heat conductivity ($l_{22} = 100$), the temperature evolution is faster and, as shown in figure 7, at the latest times of our simulations a linear profile is obtained. The domain pattern evolution, shown in figure 8, proceeds also in this case with elongated configurations perpendicular to the temperature gradient except than in the regions close to the walls. By

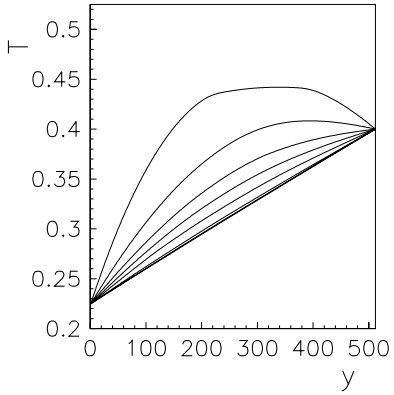

Figure 7. Temperature profiles across the system averaged along the x-direction with $T_u = 0.4$, $T_l = 0.225$ and $l_{22} = 100$ at times $t = 250$, 750, 1250, 1750, 2500, 5000, 7500, 10 000 (from top to bottom).

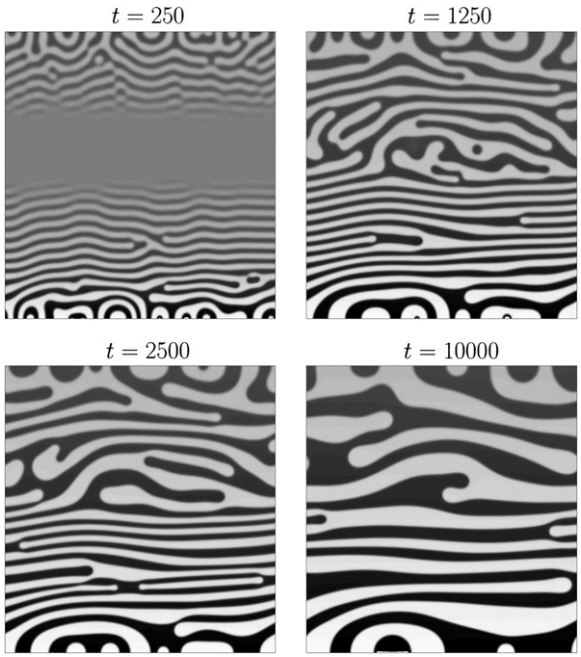

Figure 8. Contour plots of φ at consecutive times during phase separation on a system of size 512×512 with $T_u = 0.4$ and $T_l = 0.225$ and $l_{22} = 100$. Cold and hot walls are placed at the bottom and top sides, respectively. Gray scaling from white $\rightarrow$ black corresponds to maximum $\varphi \rightarrow$ minimum φ.

visual comparison with the case at lower heat conductivity, one observes that the width of domains in the vertical direction is smaller, at the same times, for higher heat conductivity. This is confirmed by the analysis of the behavior of the first momenta of the structure factor. In all the cases studied with dynamical temperature, we could not find patterns with domains elongated in the direction parallel to the temperature gradient as it appeared in the case with the fixed temperature profile.

4. Conclusions

In this paper, we have considered the dynamical equations of binary fluids where also the temperature is a dynamical quantity. The fluid mixture is described by a generic state equation with gradient contributions added to internal energy and entropy providing the standard coarse grained description of interfaces. We derived a general expression for the pressure tensor which takes into account concentration gradient terms and is consistent with other thermodynamic relations.

We considered examples of applications where contributions due the presence of the velocity field are neglected. In particular, we have studied phase separation in a system with a fixed temperature profile and in cases where the quench occurs by contact with external cold walls and the temperature evolves inside the system following the heat equation. Domain patterns are different in the two situations: in the case with dynamical temperature, domains prevalently form with interfaces perpendicular to the thermal gradient while the domains are elongated along the thermal gradient in the other case. This result is different from what was found in the simulations of [20, 21], based on different models, where the domains orientate always parallel to the thermal gradient. Instead, our results for the domain orientation are similar to those of [22] where the temperature was varied in the system with a fixed law, not coupled with the concentration field.

Concerning growth properties, in the case with a fixed thermal gradient, we measured horizontal, vertical and spherically averaged typical domain size. A power law with exponent $1/3$ was always found as in usual diffusive growth. Hopefully, in the future, effects of the velocity field will also be evaluated.

References

[1] Rowlinson J S and Widom B 1989 *Molecular Theory of Capillarity* (Oxford: Clarendon)
[2] van der Waals J D 1893 *Verh.-K. Ned. Akad. Wet., Afd. Natturkd., Eerste Reeks* **1** 56
[3] Cahn J W and Hilliard J E 1958 *J. Chem. Phys.* **28** 258
[4] Landau L D and Lifschitz E M 1958 *Statistical Physics* (Reading, MA: Addison-Wesley)
[5] Korteweg D 1901 *Arch. Neerl. Sci. Exactes Nat., Ser. II* **6** 1
[6] Yang A J M, Fleming P D and Gibbs J H 1976 *J. Chem. Phys.* **64** 3732
[7] Anderson D M, McFadden G B and Weehler A A 1998 *Annu. Rev. Fluid Mech.* **30** 139
[8] Nikolayev V S and Beysens D A 1999 *Europhys. Lett.* **47** 345
[9] Onuki A 2002 *Physica* A **314** 419
[10] Onuki A 2005 *Phys. Rev. Lett.* **94** 054501
Onuki A 2007 *Phys. Rev.* E **75** 036304
[11] Onuki A and Kanatani K 2005 *Phys. Rev.* E **72** 066304
[12] Pooley C M, Kuksenok O and Balazs A C 2005 *Phys. Rev.* E **71** 030501
[13] Antanovskii L K 1996 *Phys. Rev.* E **54** 6285
[14] Español P 2001 *J. Chem. Phys.* **115** 5392
[15] Español P and Thieulot C 2003 *J. Chem. Phys.* **118** 9109
[16] Gonnella G, Lamura A and Sofonea V 2007 *Phys. Rev.* E **76** 036703
[17] Reichl L E 1980 *A Modern Course in Statistical Physics* (London: Edward Arnold LTD)
[18] De Groot S R and Mazur P 1962 *Non-Equilibrium Thermodynamics* (Amsterdam: North-Holland)
[19] Bray A J 1994 *Adv. Phys.* **43** 357
[20] Thieulot C, Janssen L P B M and Español P 2005 *Phys. Rev.* E **72** 016714
Thieulot C and Español P 2005 *Comp. Phys. Commun.* **169** 172
[21] Jasnow D and Viñals J 1996 *Phys. Fluids* **8** 660
[22] Ball R C and Essery R L H 1990 *J. Phys.: Condens. Matter* **2** 10303